Figure Legend:

Fig.S1 Assembly of the spliceosomal complexes on ATM WT and ATM Δ exon substrates.

(A) Spliceosomal complex assembly across ATM Δ substrate alone or in presence of either 5'ss RNA oligo or U12 oligo complementary to nucleotides 11 to 28 of human U12 snRNA as a negative control.

(B) Spliceosomal complex assembly at different time points across both the ATM WT and ATM Δ single exon substrates. Quantification of the relative intensity of A-like complex assembled at different time points is plotted at the bottom of the figure.

Figure S2. IP of SR proteins following UV cross-linking.

The RNA probes used in this study (hTot, hΔ2e, ATM Δ) were obtained from the fibronectin EDA exon both in its wild-type form (hTot) and containing a deletion in its principal ESE region (hΔ2e). The UV cross-linking analysis was performed with HeLa nuclear extract. Each RNA was labeled with [α-^{32}P]UTP and then incubated with approximately 150 μg of HeLa nuclear extract before being subjected to UV cross-linking and digestion with RNase. Samples were then run on an SDS-11% PAGE gel and exposed to BioMax autoradiographic film. The electrophoretic mobility of prestained markers (Broad Range; New England Biolabs) is shown on the left figure. IP was then performed with equal amounts of each UV cross-linked sample shown in left figure with specific MAbs against different SR proteins: SF2/ASF (left, MAb 96), the phosphorylated RS domain (Middle, MAb 1H4), and SC35 (Right, anti-SC35). The mobility of the SR proteins is indicated on the left.

Figure S3. Structural determination of the ATM Δ 15-35 Del and ATM Δ 40-60 Del RNAs

Fig.S3 show the enzymatic structure determination profiles of the ATMΔ 15-35 Del and ATMΔ 40-60 Del RNAs using RNAse digestion with the S1, V1, and T1 enzymes. No enzyme was added to the RNA in a control reaction mixture (lane C). This analysis was performed on the entire RNA transcript obtained from the ATM Δ 15-35 Del and ATM Δ 40-60 Del plasmids (approx. 700 nt.). By providing an extensive background of flanking RNA molecule we have aimed to minimize any folding bias that may have derived from analyzing the pseudoexon sequence alone. The cleaved fragments were detected by performing a RT reaction using a labelled ^{32}P-end labelled antisense oligo (5'gtcaaacagaaaattcaaatccc3') and separating them in a denaturing 6% polyacrylamide gel. A sequencing reaction performed with the same RT primer was run in parallel to the cleavages in order to determine the cleavage sites (Fig.S3, lanes G, A, T, C). Squares, circles and triangles indicate S1, T1 and V1 cleavage sites. Black and white symbols indicate high and low cleavage intensity, respectively.. The observed cleavages were then compared with the ATM folding predictions by mFold (Fig.S3). The positions of the predicted SF2/ASF and hnRNPA1 binding motifs are indicated on the predicted RNA structure.

Figure S4.

RNase H digestion to inactivate U1 snRNA

In order to inactivate U1 snRNP, a small oligonucleotide (5'-ccaggtaagtat-3', U1AS oligonucleotide) was added to the reaction mixture at different concentration of as mentioned in the figure. The degree of endogenous RNase H inactivation of U1 snRNP was determined after adding different concentrations of U1AS oligonucleotide directly to 20 μL of splicing mix containing 48% HeLa nuclear extract and incubated for 30 min at 37 °C. Total RNA was then isolated by phenol/chloform extraction and ethanol precipitation. The uncleaved and cleaved forms of U1 snRNA were visualized by ethidium bromide staining. Position of the uncleaved (U1) and cleaved U1 snRNA (U1*) is shown on the right.

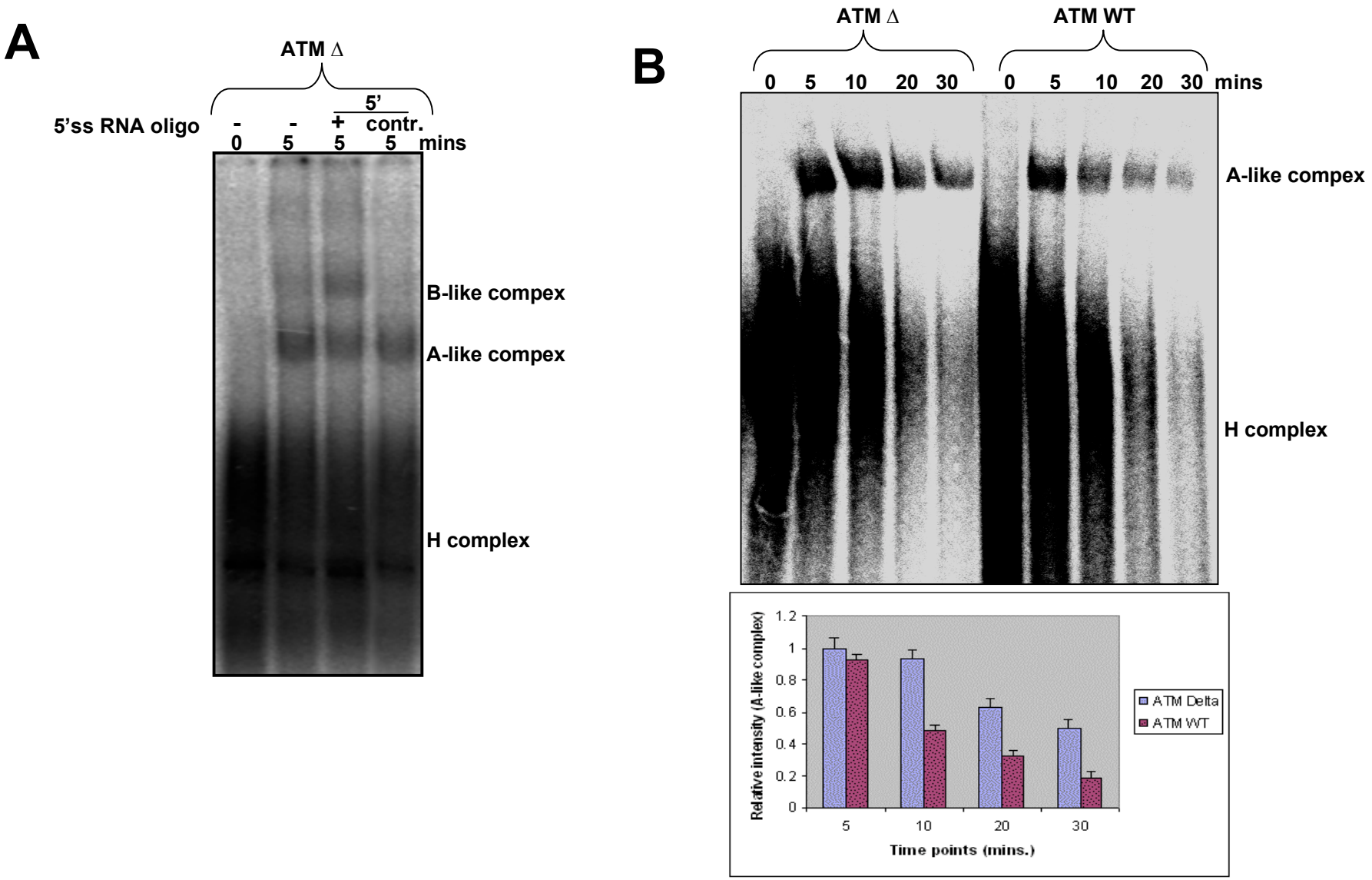

Figure S1: Assembly of the spliceosomal complexes on ATM WT and ATM Δ exon substrates.
(A) Spliceosomal complex assembly across ATM Δ substrate alone or in presence of either 5'ss RNA oligo or U12 oligo complementary to nucleotides 11 to 28 of human U12 snRNA as a negative control.
(B) Spliceosomal complex assembly at different time points across both the ATM WT and ATM Δ single exon substrates. Quantification of the relative intensity of A-like complex assembled at different time points is plotted at the bottom of the figure.

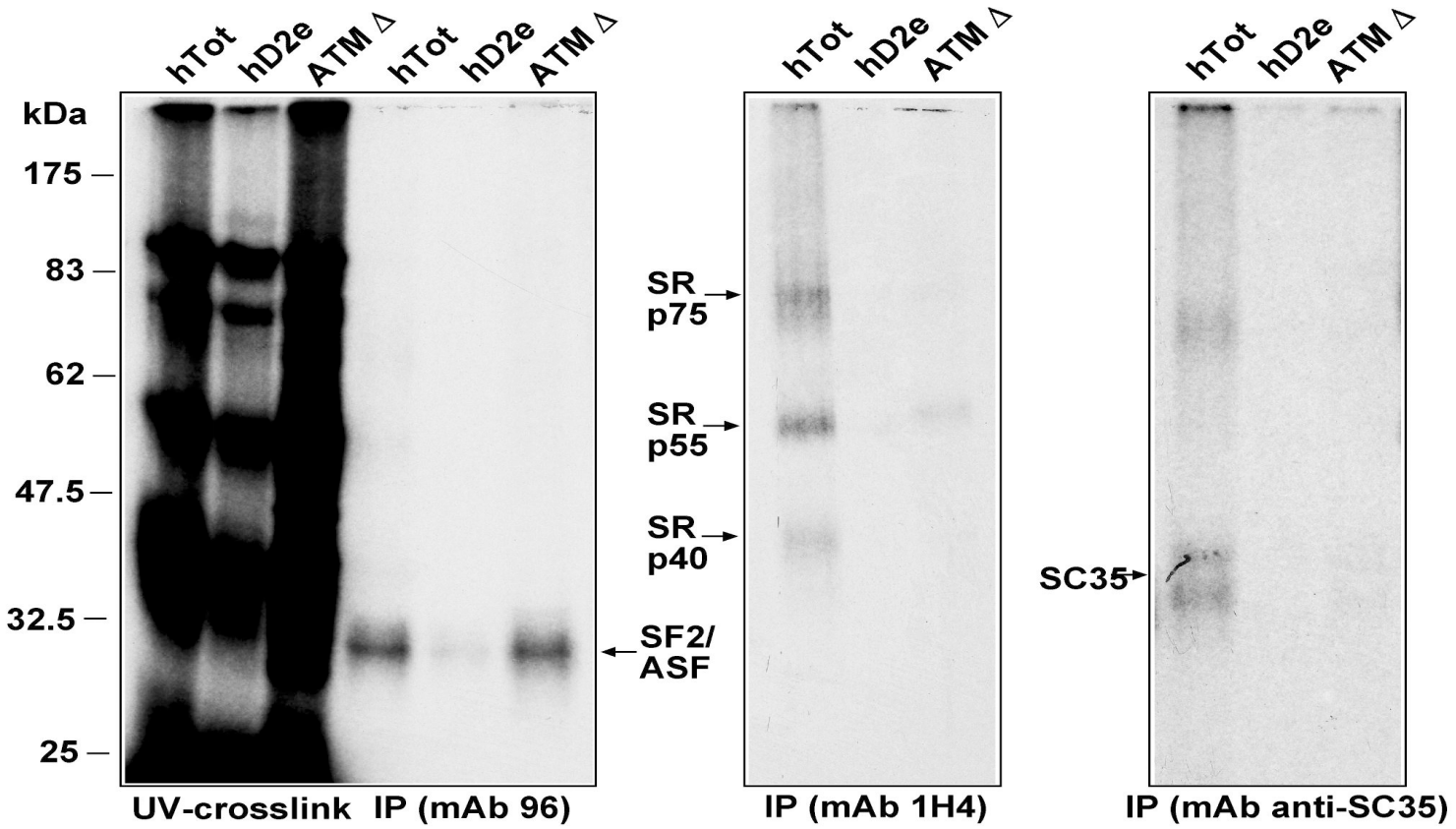

Figure S2: IP of SR proteins following UV cross-linking.
The RNA probes used in this study (hTot, hΔ2e, ATM Δ) were obtained from the fibronectin EDA exon both in its wild-type form (hTot) and containing a deletion in its principal ESE region (hΔ2e). The UV cross-linking analysis was performed with HeLa nuclear extract. Each RNA was labeled with [α-32P]UTP and then incubated with approximately 150 µg of HeLa nuclear extract before being subjected to UV cross-linking and digestion with RNase. Samples were then run on an SDS-11% PAGE gel and exposed to BioMax autoradiographic film. The electrophoretic mobility of prestained markers (Broad Range; New England Biolabs) is shown on the left figure. IP was then performed with equal amounts of each UV cross-linked sample shown in left figure with specific MAbs against different SR proteins: SF2/ASF (left, MAb 96), the phosphorylated RS domain (Middle, MAb 1H4), and SC35 (Right, anti-SC35). The mobility of the SR proteins is indicated on the left.

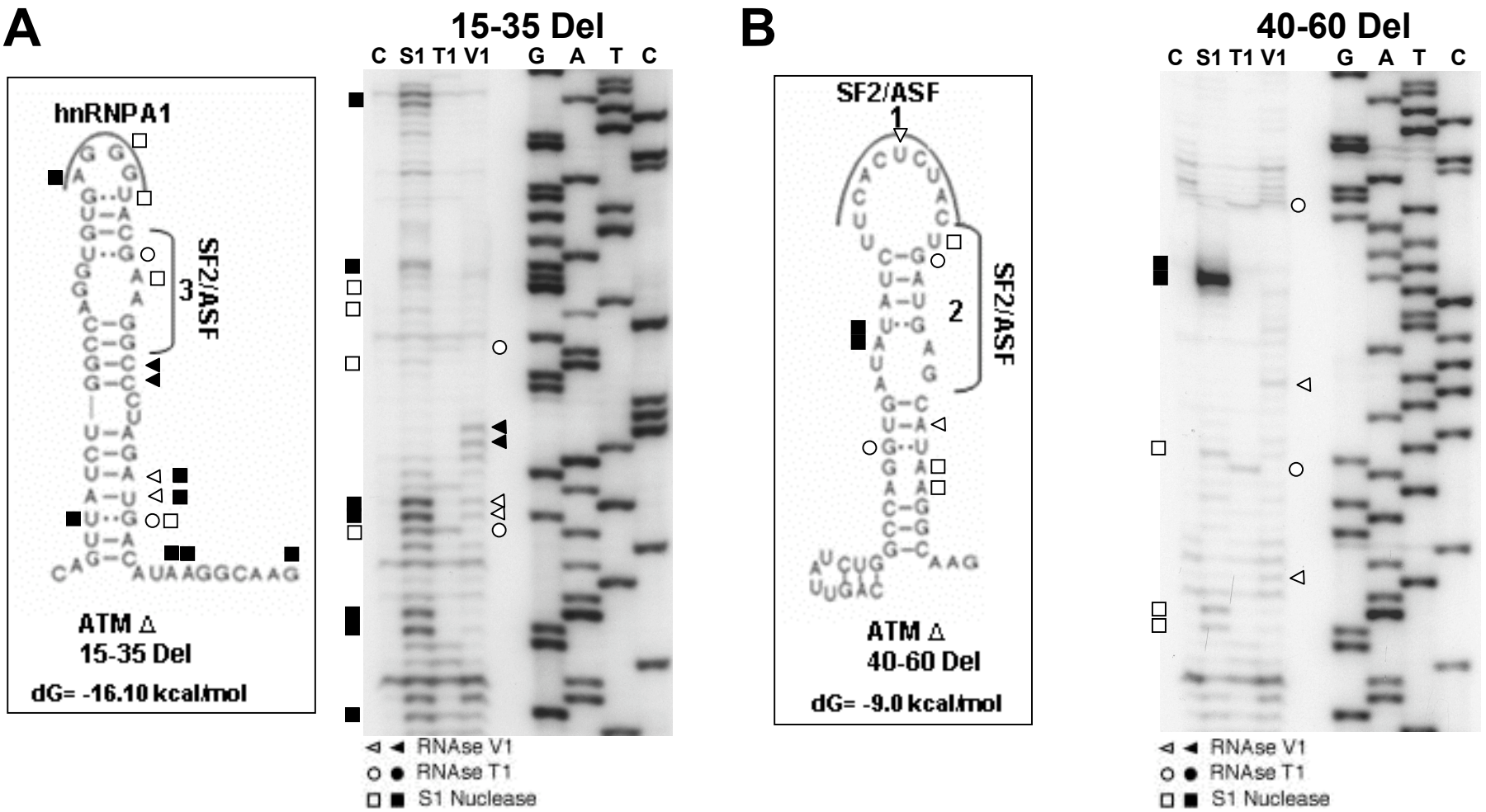

Figure S3: Structural determination of the ATM Δ 15-35 Del and ATM Δ 40-60 Del RNAs.

Fig. S3A and S3B show the enzymatic structure profiles of the ATMΔ 15-35 Del and ATMΔ 40-60 Del RNAs using RNAse digestion with the S1, V1, and T1 enzymes respectively. No enzyme was added to the RNA in a control reaction (lane C). This analysis was performed on the entire RNA transcript obtained from the ATM Δ 15-35 Del and ATM Δ 40-60 Del plasmids (approx. 700 nt.). By providing an extensive background of flanking RNA molecule we have aimed to minimize any folding bias that may have derived from analyzing the pseudoexon sequence alone. The cleaved fragments were detected by performing a RT reaction using a 32P-end labelled antisense oligo (5'gtcaaacagaaaattcaaatccc3') and separating them on a denaturing 6% polyacrylamide gel. A sequencing reaction performed with the same RT primer was run in parallel to the cleavages in order to determine the cleavage sites (Fig.S3A, S3B lanes G, A, T, C). Squares, circles and triangles indicate S1, T1 and V1 cleavage sites. Black and white symbols indicate high and low cleavage intensity, respectively. The observed cleavages were then compared with the ATM folding predictions by mFold (shown in the boxes left of each probing assay Fig.S3A, S3B). The positions of the hnRNPA1 and SF2/ASF binding motifs are indicated on the predicted RNA structure.

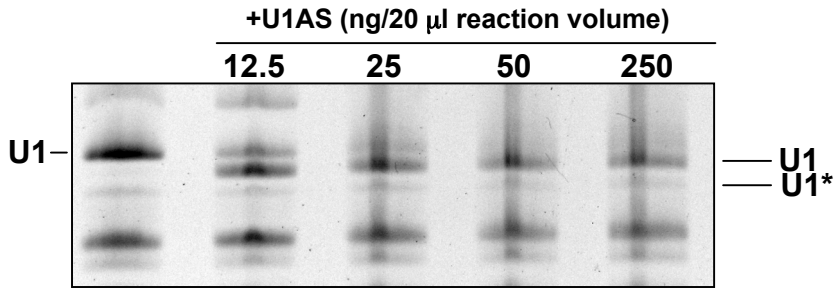

Figure S4: RNase H digestion to inactivate U1 snRNA.
In order to inactivate U1 snRNP, a small oligonucleotide (5'-ccaggtaagtat-3', U1AS oligonucleotide) was added to the reaction mixture at different concentration of as mentioned in the figure. The degree of endogenous RNase H inactivation of U1 snRNP was determined after adding different concentrations of U1AS oligonucleotide directly to 20 µL of splicing mix containing 48% HeLa nuclear extract and incubated for 30 min at 37 °C. Total RNA was then isolated by phenol/chloform extraction and ethanol precipitation. The uncleaved and cleaved forms of U1 snRNA were visualized by ethidium bromide staining. Position of the uncleaved (U1) and cleaved U1 snRNA (U1*) is shown on the right.